Desalination and Water Treatment
www.deswater.com
doi: 10.1080/19443994.2013.877854

53 (2015) 3656–3667
March

Taylor & Francis
Taylor & Francis Group

Adsorption isotherm, kinetic modeling and thermodynamics of crystal violet dye on coconut husk-based activated carbon

Aseel M. Aljeboree[a], Ayad F. Alkaim[a,*], Ammar H. Al-Dujaili[b]

[a]*Department of Chemistry, College of Science for Women, Babylon University, Hilla, Iraq*
Tel. +964 780 132 4986; email: ayad_alkaim@yahoo.com
[b]*Department of Chemistry, College of Education for Pure Science, Ibn Al-Haytham, University of Baghdad, Baghdad, Iraq*

Received 12 October 2013; Accepted 3 December 2013

ABSTRACT

The present study shows that the H_2SO_4-modified coconut husk derived activated carbon powder (CHACP) can be used as a potential adsorbent for the removal of crystal violet (CV, basic dye) from aqueous solutions. Experiments were carried out as a function of contact time, concentration, pH, mass dosage, and temperature, the equilibrium was attained in 60 min. The amount of dye uptake (mg/g) was found to increase with increase in dye concentration, pH, temperature, and contact time. The kinetics of CV on to the adsorbent can be described well by pseudo-second order > Elovich > pseudo-first order > intra-particle diffusion equation. The applicability of the isotherm's model for the present data follows the order: Freundlich > Temkin > Langmuir. Based on the calculated thermodynamic parameters such as enthalpy (ΔH°), entropy (ΔS°), activation energy (Ea), sticking probability (S^{*}), and Gibbs free energy changes (ΔG°), it is noticeable that the sorption of CV dye onto CHACP was a spontaneous and endothermic process. The morphological and chemical characteristics of the adsorbent were established by scanning electron microscopy and Fourier transform infrared spectroscopy.

Keywords: Adsorption; Coconut husk; Activated carbon; Crystal violet; Activation energy

1. Introduction

Dyes are one of the major constituents of the wastewater produced from many industries related to textile, paint, varnishes, ink, plastics, pulp, and paper. One of the famous dyes in the industry fields was crystal violet (CV), also called genetian violet is a triarylmethane dye, extensively used as a purple dye in textile industry for dyeing of cotton and silk. It also finds application in the manufacture of paints, printing inks [1,2], and is also used as an external skin disinfectant [3]. As such, a considerable amount of the colored effluents enter the natural environment and contaminates not only the environment but also fence through the entire food chain, leading to biomagnifications [4] due to its potentially potent genotoxicity, carcinogenicity, mutagenicity, and teratogenicity on exposed organisms [1]. The dye is responsible for causing heartbeat increase, vomiting, shock, cyanosis, jaundice, quadriplegia, and tissue necrosis in humans [5,6], and in extreme cases, it may also lead to respiratory and kidney

*Corresponding author.

failures and permanent injury to the cornea and conjunctiva [2,7].

Many techniques involving physical, chemical, and biological methods have been exploited to apply in treating the dye wastewater [8]. Such as photodegradation [9], coagulation flocculation [10], chemical oxidation, and biological method [11], etc. are available for the removal of dye from the wastewater. These methods can remove dyes from wastewater, but they are often expensive, inefficient, and produce secondary waste products [12].

Amongst the numerous techniques available for dye removal, adsorption has been identified to be efficient and economical for the treatment of wastewaters containing dyes, pigments, and other colorants [13,14]. Several adsorbents have shown good promise for dye removal from wastewater. Activated carbon is an effective but expensive adsorbent due to its high costs of manufacturing. This has led many workers to search for the use of cheap and efficient alternative materials. These include rice husk [15,16], peanut shell [17], eggshell waste [18,19], bottom ash [20,21], coconut husk [22], lignocellulosic waste [23], coconut shell fibre [24,25], coconut copra meal [26], coconut coir pith [27], de-oiled soya [28], hen feather waste [29,30], and coconut bunch waste [31].

Therefore, the objective of this investigation was to explore the potential of CHACP as a low cost adsorbent for the removal of CV dye from aqueous solutions. The present study describes the effects of contact time, concentration, initial solution pH, adsorbent dose, and temperature on CV adsorption rate have been investigated. Adsorption kinetics, isotherms, and thermodynamics were also evaluated and reported.

2. Experimental

2.1. Materials and methods

Coconut husk, obtained from the Hilla Market in (Babylon/Iraq), are air-dried, crushed, and screened to obtain two fractions with geometrical mean sizes ranging from 63 μm to 2.5 mm. One hundred grams of the selected fraction are impregnated with concentrated H_2SO_4 (40%) and dried by oven at 80˚C for 24 h. Then, it is activated in a hot air oven at 400˚C (2 h). The carbonized material is washed with distilled water to remove the free acid until the pH of the activated carbon reached 6.6–6.8 and dried at 105˚C. The clean biomass are mechanically ground and sifted to get a powder with particle size: <75 μm.

2.2. CV stock solution

CV, $\lambda_{max} = 590$ nm, molecular formula $C_{25}H_{30}N_3Cl$, also known as hexamethyl pararosaniline chloride, Fig. 1, was purchased from Sigma–Aldrich Chemicals. A stock solution of 1,000 mg/L CV was prepared by dissolving 1.0 g/L of the dye in deionized water. The dye solution pH was adjusted using 0.1 M HCl or 0.1 M NaOH. Fresh dilutions of the desired dye concentrations were made at the start of each experiment.

2.3. Adsorption experiments

The effect of contact time and initial concentration was studied by shaking 0.30 g/L of the adsorbent at controlled temperature and pH 6.0 at different time intervals and different initial concentrations. Adsorption kinetic experiments were done, 100 mL of CV aqueous solution of (50, 100, and 150 mg/L) in a series of 250 mL flasks, maintained at temperatures (10, 25, and 55˚C). The flasks were shaken at 120 rpm for an equilibrium time of 2 h on a shaker water bath controlling temperature. The effect of adsorbent dosage on the removal of CV was studied with different adsorbent dosages (0.005–0.20 g) in a 100 mL dye solution of 50 mg/L concentration, pH 6.0 and shaken till equilibrium time (60 min).

The effect of pH on the removal of CV was investigated over the pH range of 2.0–9.0 with 0.1 g/L of the adsorbent for 60 min in a dye solution concentration of 150 mg/L. The initial solution pH was adjusted using 0.05 M HCl or 0.05 M NaOH.

The effects of temperature on the adsorption isotherms behavior and their the data were studied by performing the adsorption experiments at various temperatures (10, 25, and 55˚C) with 0.1 g/L of the

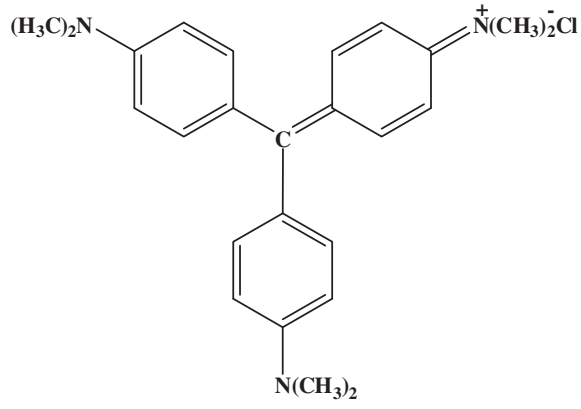

Fig. 1. Structure of crystal violet: hexamethyl pararosaniline chloride.

adsorbent and other conditions remaining constant, pH 6 and dye concentrations (10, 25, 40, 50, 75, 100, 125, 150, and 200 mg/L).

After adsorption, the adsorbent and the supernatants were separated by centrifugation at 3,500 rpm for 10 min and samples for analyses (5 mL) were withdrawn with a clinical syringe and analyzed for residual dye concentration using a UV–Visible Spectrophotometer by monitoring the absorbance changes at λ_{max} 590 nm.

2.4. Spectral analyses

The spectra of CHACP and dye loaded CHACP were recorded by an Fourier transform infrared (FTIR) spectrophotometer (FTIR 8400S) in the range of 4,500–400 cm^{-1} using a KBr disc containing 1% of the finely ground sample. The mixture was pressed into a KBr wafer under vacuum conditions and used as such for IR studies.

Scanning electron microscopy (SEM) analysis was carried out for the CHACP, and CV loaded CHACP to study the surface morphology.

The morphological features of the samples were studied by electron micrographs using SEM type FEI inspect F50 scanning electron microscope. The powder samples were placed on carbon tapes, and then coated with a thin layer of gold–palladium in an argon atmosphere using Agar Sputter Coater.

3. Results and discussion

3.1. Effect of operational variables on dye adsorption

3.1.1. Initial dye concentration/temperature of the solution/time effect

The rate of sorption of CV by CHACP was determined by contacting (50, 100, and 150 mg/L) of the CV solution (pH 6.0) with 0.3 g/L of CHACP for different intervals of time, the percentage of dye removal is given in Fig. 2(a). It was found that rate of sorption of dye were attained in the first 20 min of adsorption very highly and increased slowly to maximum at equilibrium.

When the exterior surface of CHACP reached saturation, the dye ions entered into the pores of the CHACP and were adsorbed by the interior surface of the solid particles. This process takes a relatively long time and the biosorption was slow [32].

Also, the percentage of adsorption decreased with an increase in the initial concentration and increased as the contact time prolonged. However, the increase in the initial dye concentration caused an increase in the loading capacity of the adsorbent and this may be due to the high driving force for mass at a high initial dye concentration [33]. In other words, the residual concentration of dye molecules will be higher for higher initial dye concentrations. In the case of lower concentrations, the ratio of the initial number of dye molecules to the available adsorption sites is low and subsequently the fractional adsorption becomes independent of the initial concentration [14].

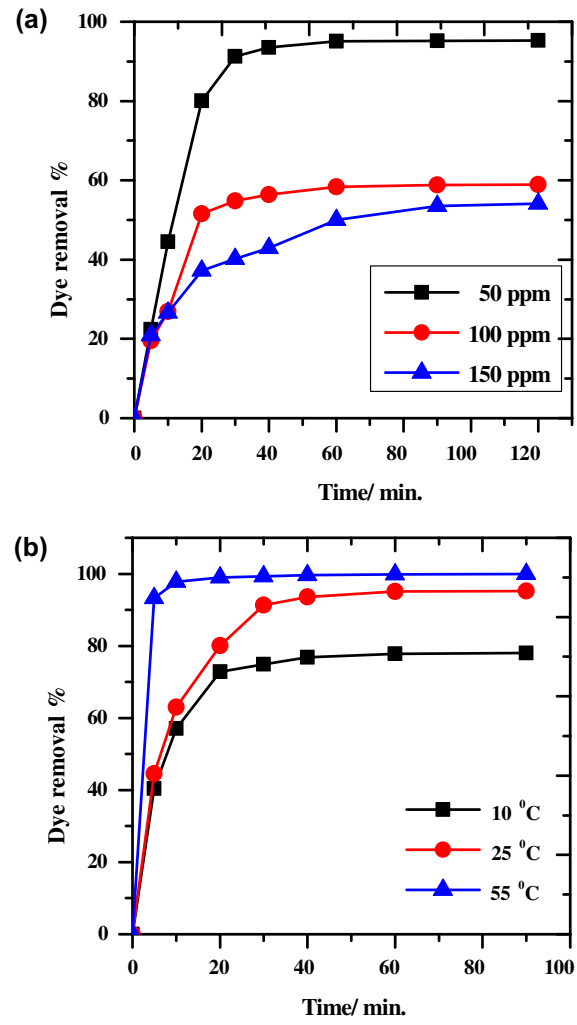

Fig. 2. (a) Effect of contact time on crystal violet adsorption on the CHACP at different initial dye concentration (Temp. 298 K, pH 6, agitation speed 120 rpm, mass of adsorbent 0.3 g/L). (b) Effect of contact time on crystal violet adsorption on the CHACP at different solution temperature (initial crystal violet 50 mg/L, pH 6, agitation speed 120 rpm, and mass of adsorbent 0.3 g/L).

The rate of sorption of CV by CHACP was determined by contacting at 10, 25, and 55℃ of the CV solution (50 mg/L, pH 6.0), with 0.3 g/L CHACP for different intervals of time, for estimating the effect of

solution temperature on dye removal efficiency and the percentage of dye removal is given in Fig. 2(b). It was found that rate of sorption of dye was attained in the first 20 min of adsorption very highly and increased slowly to maximum at equilibrium. This decline is due to decrease in the total adsorption surface area and less available binding sites [34]. Similar results have been reported in literature for adsorption of CV onto coniferous pinus bark powder [35].

As depicted in Fig. 2(b), the percentage removal of dye increased with increasing temperature, this observed trend in an increased dye removal capacity with increasing temperature suggests that adsorption of CV by CHACP is kinetically controlled by an endothermic process.

3.1.2. Adsorbent dosage

One of the parameters that strongly affect sorption capacity is the quantity of the contacting sorbent in the liquid phase because it determines the capacity of adsorbent for a given initial concentration of dye solution [36].

The effect of CHACP dosages on the amount of dye adsorbed was investigated by contacting 100 mL of dye solution with an initial dye concentration of 50 mg/L for the adsorbent, for a contact time of 60 min at a temperature of 25 ± 0.5˚C, a shaking speed of 120 rpm and optimum pH of 6.0. Different amounts of adsorbents (0.005, 0.01, 0.025, 0.05, 0.075, 0.1, 0.125, 0.150, and 0.200 g) were added. After equilibrium, the samples were allowed to settle for sometime after which the supernatant solutions were collected, centrifuged and analyzed. Results are shown in Fig. 3. The percentage of dye removal increased with an increase in adsorbent dosage. For instance, an increase from 29.1 to 99.5% was observed when the dosage increased from 0.005 to 0.075 g. When the adsorbent dosage was doubled from 0.10 to 0.20 g, dye removal was only 0.3% indicating that adsorption was almost complete with 0.10 g of the adsorbent at 50 mg/L of dye concentration.

It was obvious from Fig. 3 that the decrease in sorption capacity with increasing dose of adsorbent at constant dye concentration and volume may be attributed to saturation of adsorption sites due to particulate interaction such as aggregation [37].

The increase in the percentage of dye removal with adsorbent dose could be attributed to an increase in the adsorbent surface area, augmenting the number of adsorption sites available for adsorption, as already reported [14].

3.1.3. Effect of solution pH on dye adsorption

The solution pH is an important monitoring parameter governing an adsorption process. It not only influences the degree of ionization of the adsorbate but also the surface charge of the adsorbent species present in the solution. Effect of pH on adsorption was studied using 150 mg/L dye concentration, pH 2–9 at 25˚C, results are given in Fig. 4. From Fig. 4, the dye uptake (q_e) was found to increase with increasing pH.

Lower adsorption of CV at acidic pH is probably due to the presence of excess H^+ ions competing with

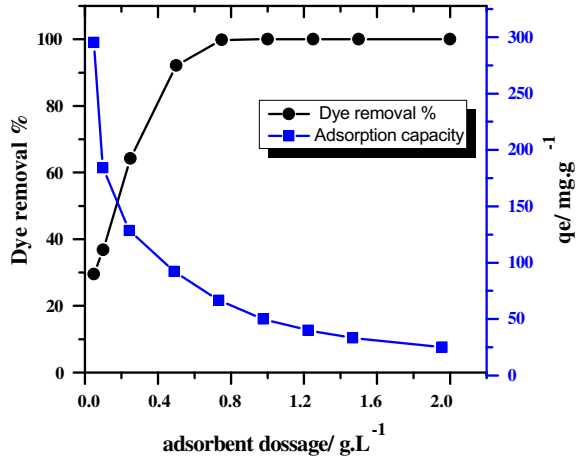

Fig. 3. Effect of adsorbent dosage on the percent removal and amount of adsorbed CV dye onto CHACP (crystal violet initial concentration = 50 mg/L, Temp. = 25˚C, contact time 1 h, and pH of solution 6).

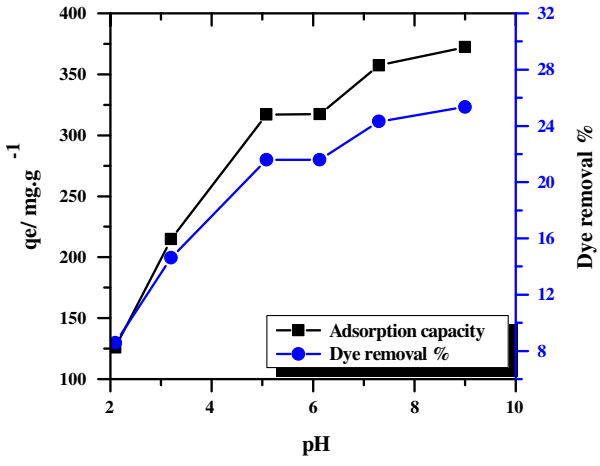

Fig. 4. Effect of solution pH on the percent removal and amount of adsorbed CV dye onto CHACP (crystal violet initial concentration = 150 mg/L, Temp. = 25˚C, contact time 2 h, and mass of adsorbent 1 g/L).

the cation groups on the dye for adsorption sites [7]. At higher pH, the surface of CHACP may get negatively charged, which enhances the positively charged dye cations through electrostatic forces of attraction [7].

3.2. Adsorption kinetics

The kinetics of adsorption describes the rate of adsorbate uptake on adsorbent and it controls the equilibrium time. The kinetic parameters are helpful for the prediction of adsorption rate, which gives important information for designing and modeling the processes [38].

In this study, the adsorption kinetics data are analysed using four common models, specifically, the pseudo-first order [39], pseudo-second order [40], Elovich equation [41], and intra-particle diffusion [42].

A simple kinetic analysis of adsorption is Lagergren (pseudo-first order) in the form:

$$q_t = q_e[1 - \exp(k_f t)] \tag{1}$$

where q_t is the amount of adsorbate adsorbed at time t (mg/g), q_e is the adsorption capacity in the equilibrium (mg/g), k_f is the pseudo-first-order rate constant (min^{-1}), and t is the contact time (min).

Lagergren equation represents the pseudo-first-order kinetics for the whole adsorption reaction, with a one-partial order with respect to the free concentration sites and a zero-partial order with respect to the solute in the solution.

A pseudo-second-order equation based on adsorption equilibrium capacity may be expressed in the form:

$$q_t = \frac{k_s q_e^2 t}{1 + k_s q_e t} \tag{2}$$

where k_s is the pseudo-second-order rate constant (g/mg min), the initial sorption rate (h_o, expressed in mg/g min) can be obtained when t approaches to zero Eq. (3):

$$h_0 = k_s q_e^2 \tag{3}$$

The Elovich equation is for general application to chemisorption. The equation has been applied satisfactorily to some chemisorption processes and has been found to cover a wide range of slow adsorption rates. The same equation is often valid for systems in which the adsorbing surface is heterogeneous, and is formulated as:

$$q_t = \left(\frac{1}{\beta}\right)\ln(\propto \cdot \beta) + \left(\frac{1}{\beta}\right)\ln(t) \tag{4}$$

where $\propto$ is the chemisorptions rate constant (mg/g min)

The intra-particle diffusion model based on the theory proposed by Weber and Morris [42] was used to identify the diffusion mechanism. According to this theory, the adsorbate uptake q_t varies almost proportionally with the square root of the contact time, $t_{½}$ rather than t, Eq. (5):

$$q_t = k_{id}\sqrt{t} + I \tag{5}$$

where I is the intercept and k_{id} (mg/g min) is the intra-particle diffusion rate constant.

The fitted parameters of adsorption kinetics of CV (50, 100, and 150 mg/L) at different temperatures 10, 25, and 55°C (Table 1) were calculated from the non-linear regressions of the integrated Eqs. (1), (2), (4), and (5). The profiles of the fitted curve of the experimental kinetics of CV (100 mg/L) displayed in Fig. 5 were very similar to the ones of fitted kinetic plots at CV (50 and 150 mg/L) (figures not shown).

From Fig. 5, it was found that the uptake of the dye by the sorbent adsorption capacity increases with increasing temperature from 10 to 55°C, indicating that the adsorption is an endothermic process [43].

An increasing number of molecules may also acquire sufficient energy to undergo an interaction with active sites at the surface [44], also the increase in the adsorption may be a result of increase in the mobility of the dye with increasing temperature [45]. The best correlation for the system provided by the pseudo-second-order model suggests that chemical sorption involving valency forces through sharing or exchanging of electrons between adsorbent and adsorbate might be significant. A similar phenomenon was also observed in the adsorption of CV on wheat straw [46].

3.3. Adsorption isotherms modeling

Adsorption data are most commonly represented by the equilibrium isotherm value, which is a plot of the quantity of the sorbate removed per unit sorbent (q_e) as the solid-phase concentration of the sorbent against the concentration of the sorbate in the liquid phase (C_e).

Table 1
Pseudo-first-order, pseudo-second-order, chemisorption, and intraparticle diffusion model constants and correlation coefficients for CV adsorption onto CHACP at pH 6, particle size 75 μm, mass catalyst 0.03 mg, and agitation speed 120 rpm

		Initial dye concentration (50 mg/L)			Initial dye concentration (100 mg/L)			Initial dye concentration (150 mg/L)		
Kinetic model	Parameter	T/283 K	T/298 K	T/323 K	T/283 K	T/298 K	T/323 K	T/283 K	T/298 K	T/323 K
Pseudo-first order	k_f	0.142	0.115	0.557	0.077	0.095	0.318	0.14006	0.09102	0.31854
	q_e	128.2855	156.1966	165.357	175.9027	194.8431	249.3610	215.4026	229.4700	261.7038
	R^2	0.9987	0.9942	0.99977	0.88447	0.99785	0.97209	0.98023	0.96562	0.97114
Pseudo-second order	ks	0.1878	0.13949	2.63825	0.07262	0.10457	0.60097	0.18238	0.10219	0.60502
	q_e	145.7184	167.8506	182.2054	224.2203	234.7971	265.1940	245.9373	276.2942	278.2264
	h_o	3987.717	4630.902	74329.64	3650.953	5764.911	42264.9	11031.28	7801.033	46834.58
	R^2	0.97238	0.98963	0.96184	0.76708	0.96531	0.79874	0.98743	0.96201	0.80677
Chemisorption	α	94.127	65.345	5.98E(18)	28.023	1737.49	16,963	150.454	65.634	17015.98
	β	0.03888	0.027823	0.246064	0.017827	0.01954	0.03961	0.022762	0.017309	0.03775
	R^2	0.97568	0.98688	0.9991	0.88995	0.97269	0.99648	0.99659	0.99486	0.99821
Intra-particle diffusion	k_{id}	16.72381	20.95723	32.8345	25.18684	26.64599	30.02313	28.60493	31.48072	31.55103
	I	24.91279	23.23567	17.45328	5.70061	20.44345	78.87116	39.68738	23.33808	82.66436
	R^2	0.81552	0.88103	0.45702	0.82534	0.89011	0.66193	0.86483	0.95387	0.66498

At position of dynamic equilibrium of adsorption process, there arise a require to determine the adsorbate spreading between the liquid phase and solid phase; this information can be obtained through adsorption isotherms studies [47].

Several isotherm models have been used to predict validity of the experimental data. In the present study, three of the most commonly used models, namely the Langmuir, Freundlich, and Temkin isotherms were used to describe the adsorption equilibrium.

The non-linear form of the Langmuir isotherm model [48] is given as:

$$q_e = \frac{q_{max} K_L C_e}{1 + K_L C_e} \tag{6}$$

where K_L (L/mg) is the Langmuir adsorption constant related to the energy of adsorption, q_{max} and q_e (mg/g) are the maximum and equilibrium adsorption capacity, respectively. Langmuir constants generated from adsorption data plot of q_e against C_e, shown in Fig. 6, are summarized in Table 2.

The Freundlich isotherm is based on the premise that adsorption occurs on rare heterogeneous surface sites with different energies of adsorption and are also non-identical. The non-linear form of the Freundlich isotherm was used to investigate the adsorption process adherence to the model [49]:

$$q_e = k_f C_e^{1/n} \tag{7}$$

k_f can be defined as the adsorption or distribution coefficient and represents the quantity of dye adsorbed onto adsorbent for unit equilibrium concentration, $1/n$ is the heterogeneity factor, and n is a measure of the deviation from linearity of adsorption. Its value indicates the degree of non-linearity between solution concentration and adsorption as follows: if the value of n is equal to unity, the adsorption is linear; if the value is below unity, this implies that adsorption process is chemical; if the value is above unity, adsorption is a favorable physical process [50]. The values of the model parameters obtained from the plot of q_e against C_e shown in Fig. 6 are presented in Table 2.

The non-linearized form of Temkin isotherm [51] is represented by Eq. (8):

$$q_e = \frac{RT}{b} \log(K_T C_e) \tag{8}$$

where b Temkin constant related to the heat of adsorption(kJ/mol), R gas constant (8.314 J/mol K), T temperature (K), and K_T Empirical Temkin constant related to the equilibrium binding constant related to the maximum binding energy (L/mg).

The adsorption data can be analyzed according to Eq. (8). A plot of the q_e vs. log C_e shown in Fig. 6 enables the determination of the isotherm constants K_T and b shown in Table 2.

All the three isotherms under study described the adsorption of CV on CHACP. The best fit of isotherm

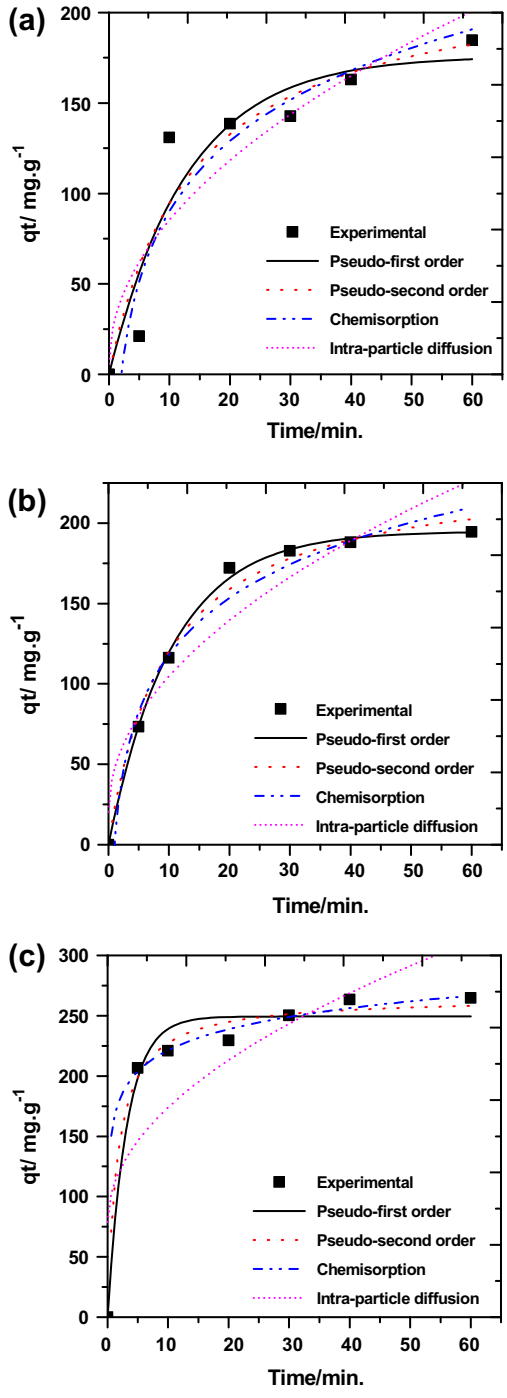

Fig. 5. Different adsorption kinetics models fit for adsorption of CV dye on CHACP at (a) 10℃, (b) 25℃, and (c) 55℃. (Experiment conditions: pH 6, mass dosage 0.3 g/L, and initial dye conc. 100 ppm).

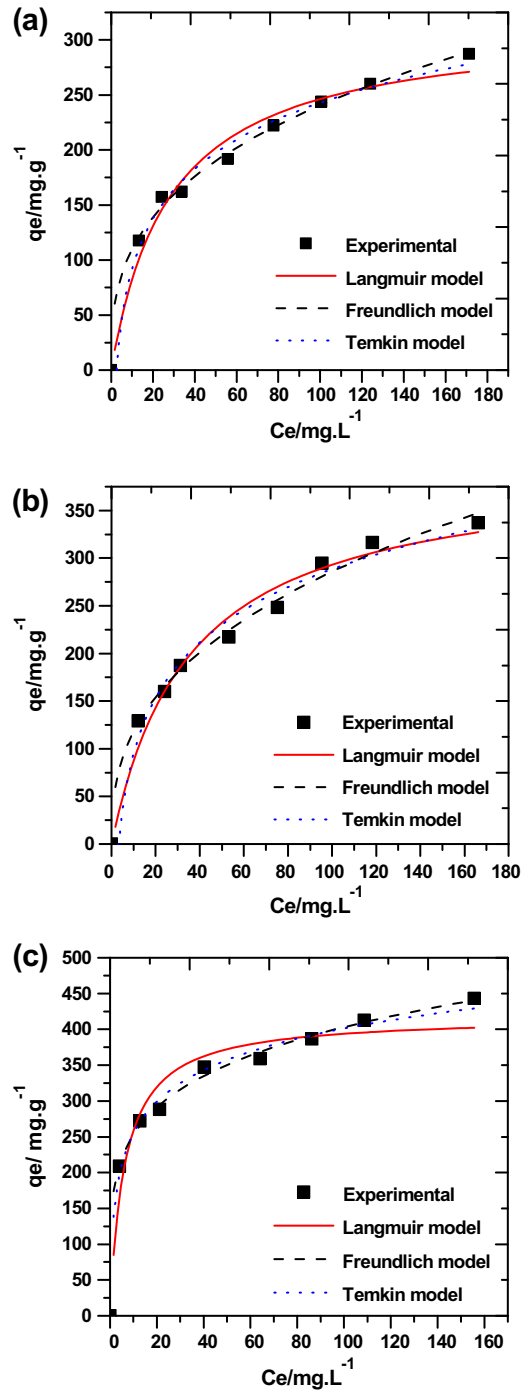

Fig. 6. Different adsorption isotherm models fit for adsorption of CV dye on CHACP at (a) 10℃, (b) 25℃, and (c) 55℃. (Experiment conditions: pH 6 and mass dosage 0.1 g/L).

was selected based on the highest correlation coefficient (R^2) value (closer to unity) which describes the fitness of the isotherm to the experimental data.

As observed from Table 2, although the equilibrium data fitted well to the Langmuir, Freundlich, and Temkin adsorption isotherm models, the Freundlich

Table 2
Langmuir, Freundlich, and Temkin model isotherms parameters for CV adsorbed on the surface of CHACP, in the presence of different temperatures

Isotherm models	Parameters	T/283 K	SE	T/298 K	SE	T/323 K	SE
Langmuir	q_m (mg/g)	315.860	16.987	396.977	25.735	418.068	19.479
	K_L (L/mg)	0.028	0.006	0.035	0.005	0.162	0.044
	R^2	0.9400		0.9434		0.8422	
Freundlich	K_F	48.803	4.7108	50.062	2.6959	158.728	5.408
	$1/n$	0.384	0.022	0.341	0.0120	0.202	0.008
	R^2	0.9928		0.9825		0.9908	
Temkin	B (J/mole)	83.967	5.904	65.487	3.572	63.374	3.248
	K_T	0.311	0.064	0.408	0.072	5.615	1.581
	R^2	0.9910		0.9829		0.9939	

and Temkin models exhibited a slightly better fit to the adsorption data than the Langmuir model. The increase in values at higher temperatures suggests that the adsorption process was favorable at higher temperatures. In general, $n > 1$ illustrates that adsorbate is favorably adsorbed on an adsorbent. In particular, the value of (n) is significantly higher than unity at all the temperatures studied.

The Temkin isotherm takes into account the effects of the interaction of the adsorbate and the adsorbing species. By ignoring the extremely low and large concentration values, the model assumes that the heat of adsorption (a function of temperature) of all of the molecules in the layer would decrease linearly rather than logarithmically with coverage due to adsorbate–adsorbent interactions [52].

An accepted fit of the Langmuir model showed that there was monolayer coverage of CV on the adsorbent surface.

The favorability of the adsorption (R_L) was evaluated from the parameters of the Langmuir adsorption isotherm model. The R_L can calculate from the following equation [45]:

$$R_L = \frac{1}{1 + K_L C_0} \tag{9}$$

where K_L is the Langmuir constant (L/mg) and C_0 is the initial concentration of dye. The R_L can vary: for $R_L > 1$, the adsorption is unfavorable; $R_L = 1$, the adsorption is Linear condition; the adsorption is favorable when $0 < R_L < 1$; and $R_L = 0$ is for irreversible conditions. The value of R_L for the sorption of CV onto CHACP is shown in Fig. 7, which indicates that sorption of CV on CHACP was "favorable". According to Fig. 7, the R_L values for CHACP were achieved between 1 and 0 indicating favorable adsorption of

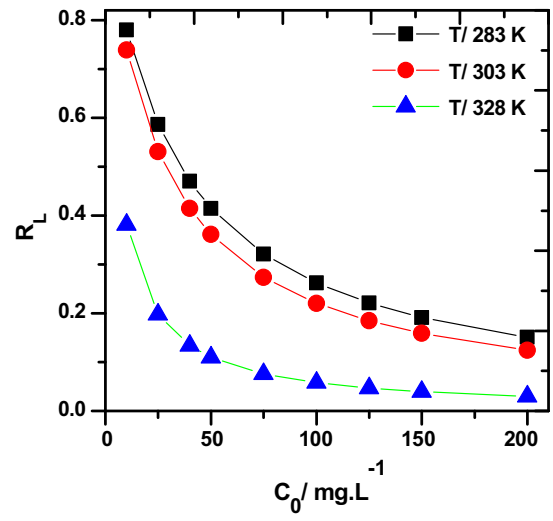

Fig. 7. Value of separation factor R_L for adsorption of crystal violet by CHACP at different temperatures.

CV onto CHACP surface. The monolayer coverage obtained from this is 396.97 mg g^{-1}, considering good for a comparison with previous data in literatures [1,35,36,46,53–57].

3.4. Thermodynamic parameters

The understanding and prediction of thermodynamic parameters are the most suited conditions for the evaluation of an adsorption process. The thermodynamic parameters were developed under the assumption that the sorbate molecules are absorbed into a porous adsorbent with a constant void fraction, providing a uniform distribution on the surface [58]. The parameters chosen in this study are change in enthalpy (ΔH°), entropy (ΔS°), and Gibbs free energy

change (ΔG°). The experimental values obtained from the following equations inform whether the adsorption process was spontaneous or non-spontaneous [59].

$$\ln(K_d) = \ln\left(\frac{C_a}{C_e}\right) = -\frac{\Delta G^{\circ}}{RT} \quad (10)$$

$$\ln(K_d) = \frac{\Delta S^{\circ}}{R} - \frac{\Delta H^{\circ}}{RT} \quad (11)$$

where K_d is the equilibrium constant, C_a is the amount of CV adsorbed at equilibrium (mg/L), C_e is the concentration of CV remaining in the solution at equilibrium (mg/L), T is the solution temperature (K), and R is the perfect gas constant (8.314 J/mol K). The isosteric enthalpy ΔH° and entropy ΔS° of adsorption were also calculated from the slope and the intercept of the plot of $\ln(K_d)$ vs. $1/T$, respectively, using the equation: $\Delta G^{\circ} = \Delta H - T\Delta S^{\circ}$ (figure not shown).

Results are shown in Table 3, that indicates that the adsorption process was endothermic in nature and the magnitude of adsorption supports the formation of partial chemical processes that are involved during the removal process [60]. The negative value of the Gibbs free energy change (ΔG°) reveals that the adsorption process was spontaneous in nature [61] and the decreasing value of ΔG° with increasing temperature shows the spontaneous nature of the adsorption of CV dye. The entropy change ΔS° shows positive value, this confirms that the increasing randomness between the solid–solution interfaces during the adsorption process, probably due to the desorption of solvent molecules prior to CV dye adsorption [59].

This is the normal consequence of the combination of physical adsorption, which takes place through electrostatic interactions. In order to further support the assertion that physical adsorption is the predominant mechanism, the values of the activation energy (E_a) and sticking probability (S^*) were estimated from the experimental data. They were calculated using a modified Arrhenius type equation related to surface coverage (θ) as follows [62]:

$$S^* = (1-\theta)e^{-\left(\frac{E_a}{RT}\right)} \quad (12)$$

The sticking probability (S^*) value concern to adsorbate–adsorbent system under investigation. Its value lies in the range $0 < S^* < 1$ and is dependent on the temperature of the system. The parameter (S^*) indicates the measure of the potential of an adsorbate to remain on the adsorbent indefinite. The surface coverage (θ) can be calculated from Eq. (13):

$$\theta = \left(1 - \frac{C_e}{C_0}\right) \quad (13)$$

The activation energy and sticking probability are shown in Table 3, from a plot of $\ln(1-\theta)$ vs. $1/T$ (figure not shown).

The magnitude of activation energy gives an idea about the type of adsorption which is mainly physical or chemical. Low activation energies (<40 kJ mol^{-1}) are characteristics for physical adsorption, while higher activation energies (>40 kJ mol^{-1}) suggest chemical adsorption [7]. The activation energy obtained for the adsorption of CV onto CHACP indicates that the adsorption process is chemisorption.

3.5. Structural characterization by infrared spectroscopy and scan electron microscopy analysis

The adsorption process is mainly influenced by the presence of functional groups on the surface of the adsorbent material. If the surface of the adsorbent attains positive charge, then that adsorbent adsorbs anionic dyes; whereas, if the surface of the adsorbent attains negative charge, then it adsorbs cationic dyes [60]. This phenomenon of adsorption mainly depends on the presence of surface charges of an adsorbent. The presence of various functional groups in the adsorbent material was identified with

Table 3
Thermodynamic functions ΔG, ΔS, ΔH, E_a, and S^* of CV dye adsorbed on the CHACP

T/K	K_d	ΔG^o (kJ/mol)	ΔH^o (kJ/mol)	ΔS^o (J/K.mol)	S^*	E_a (kJ/mol)
283	2854.759	−18.7211	11.86574	107.7328	0.1838	116.7347
298	3302.264	−20.0742				122.922
328	5602.731	−23.5367				135.2967

FTIR in the range of 4,000–400 cm^{-1}. The FTIR spectrum of CHACP (figure not shown) displays a number of absorption peaks, indicating that many functional groups of the adsorbent may be involved in the adsorption. The wide band in the region (3,420–3,680 cm^{-1}) is attributed to the hydroxyl (–OH) groups (libber and intermolecular hydrogen band). The band at 1,599 cm^{-1} indicates the presence of groups (C–H and C=C), while CV dye loaded CHACP shows peaks at 3,550, 2050, 1,500, and 960 cm^{-1}.

SEM technique was applied in order to confirm the adsorption of CHACP on CV dye, the SEM micrographs of CHACP samples before and after adsorption of CV dye (figure not shown). SEM enables a direct observation of any surface microstructure changes in the samples that would have occurred due to the adsorption of CV dye. Some slight differences at the micrographs are noticeable. The number and shape of cracks and attached fine particles over the carbon surface clearly differ before and after adsorption. Minor decrease in the size of the particles after adsorption is apparent. However, the effect that would cause vast changes in the pore structure of CHACP during adsorption is not present in this case.

4. Conclusions

The present study shows that the coconut husk activated carbon powder (CHACP) can be used as a potential adsorbent for the removal of CV dye from aqueous solutions. The operational parameters such as pH, adsorbent dose, contact time, and temperature, were found to have an effect on the adsorption efficiency of CHACP. The adsorption was highly dependent on reaction temperature and solution pH. The dye was optimally adsorbed at pH 9. The calculated thermodynamic parameters showed the endothermic and spontaneous nature of the adsorption process. The applicability of the three isotherm models for the present data follows the order: Freundlich > Temkin >> Langmuir. The kinetics of CV onto the adsorbent can be described well by pseudo-second order > Elovich > pseudo-first order > Intra-particle diffusion equation. The overall rate of dye uptake was found to be controlled by external mass transfer at the beginning of adsorption, while intra-particle diffusion controlled rate of adsorption at a later stage. FTIR analysis showed that the main functional sites taking part in the sorption of CV included carboxyl and hydroxyl groups.

References

[1] S. Senthilkumaar, P. Kalaamani, C.V. Subburaam, Liquid phase adsorption of crystal violet onto activated carbons derived from male flowers of coconut tree, J. Hazard. Mater. 136 (2006) 800–808.

[2] A. Mittal, J. Mittal, A. Malviya, D. Kaur, V. Gupta, Adsorption of hazardous dye crystal violet from wastewater by waste materials, J. Colloid Interface Sci. 343 (2010) 463–473.

[3] M. Saji, S. Taguchi, K. Uchiyama, E. Osono, N. Hayama, H. Ohkuni, Efficacy of gentian violet in the eradication of methicillin-resistant *Staphylococcus aureus* from skin lesions, J. Hosp. Infect. 31 (1995) 225–228.

[4] S. Karcher, A. Kornmüller, M. Jekel, Anion exchange resins for removal of reactive dyes from textile wastewaters, Water Res. 36 (2002) 4717–4724.

[5] W. Ma, X. Song, Y. Pan, Z. Cheng, G. Xin, B. Wang, X. Wang, Adsorption behavior of crystal violet onto opal and reuse feasibility of opal-dye sludge for binding heavy metals from aqueous solutions, Chem. Eng. J. 193–194 (2012) 381–390.

[6] A. Kunz, H. Mansilla, N. Durán, A degradation and toxicity study of three textile reactive dyes by ozone, Environ. Technol. 23 (2002) 911–918.

[7] S. Chakraborty, S. Chowdhury, P.D. Saha, Adsorption of crystal violet from aqueous solution onto NaOH-modified rice husk, Carbohydr. Polym. 86 (2011) 1533–1541.

[8] T. Robinson, G. McMullan, R. Marchant, P. Nigam, Remediation of dyes in textile effluent: A critical review on current treatment technologies with a proposed alternative, Bioresour. Technol. 77 (2001) 247–255.

[9] A.N. Ejhieh, M. Khorsandi, Photodecolorization of Eriochrome Black T using NiS–P zeolite as a heterogeneous catalyst, J. Hazard. Mater. 176 (2010) 629–637.

[10] Y. Zhou, Z. Liang, Y. Wang, Decolorization and COD removal of secondary yeast wastewater effluents by coagulation using aluminum sulfate, Desalination 225 (2008) 301–311.

[11] O. Türgay, G. Ersöz, S. Atalay, J. Forss, U. Welander, The treatment of azo dyes found in textile industry wastewater by anaerobic biological method and chemical oxidation, Sep. Purif. Technol. 79 (2011) 26–33.

[12] B.K. Nandi, A. Goswami, M.K. Purkait, Removal of cationic dyes from aqueous solutions by kaolin: Kinetic and equilibrium studies Appl. Clay Sci. 42 (2009) 583–590.

[13] M. Asgher, N.H. Bhatti, Removal of reactive blue 19 and reactive blue 49 textile dyes by citrus waste biomass from aqueous solution: Equilibrium and kinetic study, Can. J. Chem. Eng. 90 (2012) 412–419.

[14] B. Hayati, N.M. Mahmoodi, Modification of activated carbon by the alkaline treatment to remove the dyes from wastewater: mechanism, isotherm and kinetic, Desalin. Water Treat. 47 (2012) 322–333.

[15] V.K. Gupta, A. Mittal, R. Jain, M. Mathur, S. Sikarwar, Adsorption of Safranin-T from wastewater using waste materials – Activated carbon and activated rice husks, J. Colloid Interface Sci. 303 (2006) 80–86.

[16] U.R. Lakshmi, V.C. Srivastava, I.D. Mall, D.H. Lataye, Rice husk ash as an effective adsorbent: Evaluation of

adsorptive characteristics for Indigo Carmine dye, J. Environ. Manage. 90 (2009) 710–720.
[17] M.S. Tanyildizi, Modeling of adsorption isotherms and kinetics of reactive dye from aqueous solution by peanut hull, Chem. Eng. J. 168 (2011) 1234–1240.
[18] H. Daraei, A. Mittal, M. Noorisepehr, F. Daraei, Kinetic and equilibrium studies of adsorptive removal of phenol onto eggshell waste, Environ. Sci. Pollut. Res. 20 (2013) 4603–4611.
[19] H. Daraei, A. Mittal, M. Noorisepehr, J. Mittal, Separation of chromium from water samples using eggshell powder as a low-cost sorbent: Kinetic and thermodynamic studies, Desalin. Water Treat. (2013) 1–7.
[20] J. Mittal, D. Jhare, H. Vardhan, A. Mittal, Utilization of bottom ash as a low-cost sorbent for the removal and recovery of a toxic halogen containing dye eosin yellow, Desalin. Water Treat. (2013) 1–12. 10.1080/19443994.2013.803265
[21] V.K. Gupta, A. Mittal, D. Jhare, J. Mittal, Batch and bulk removal of hazardous colouring agent Rose Bengal by adsorption techniques using bottom ash as adsorbent, RSC Adv. 2 (2012) 8381–8389.
[22] A. Mittal, R. Jain, J. Mittal, M. Shrivastava, Adsorptive removal of hazardous dye quinoline yellow from waste water using coconut-husk as potential adsorbent, Fresen Environ. Bull. 19 (2010) 1–9.
[23] S. Noreen, H.N. Bhatti, S. Nausheen, S. Sadaf, M. Ashfaq, Batch and fixed bed adsorption study for the removal of Drimarine Black CL-B dye from aqueous solution using a lignocellulosic waste: A cost affective adsorbent, Ind. Crops Prod. 50 (2013) 568–579.
[24] S. Babel, T.A. Kurniawan, Cr(VI) removal from synthetic wastewater using coconut shell charcoal and commercial activated carbon modified with oxidizing agents and/or chitosan, Chemosphere 54 (2004) 951–967.
[25] D.A. de Sousa, E. de Oliveira, M.C. Nogueira, B.P. Espósito, Development of a heavy metal sorption system through the PS functionalization of coconut (*Cocos nucifera*) fibers, Bioresour. Technol. 101 (2010) 138–143.
[26] Y. Ho, A.E. Ofomaja, Biosorption thermodynamics of cadmium on coconut copra meal as biosorbent, Biochem. Eng. J. 30 (2006) 117–123.
[27] C. Namasivayam, M.D. Kumar, K. Selvi, R.A. Begum, T. Vanathi, R.T. Yamuna, 'Waste' coir pith – A potential biomass for the treatment of dyeing wastewaters, Biomass Bioenergy 21 (2001) 477–483.
[28] A. Mittal, D. Jhare, J. Mittal, Adsorption of hazardous dye eosin yellow from aqueous solution onto waste material de-oiled soya: Isotherm, kinetics and bulk removal, J. Mol. Liq. 179 (2013) 133–140.
[29] J. Mittal, V. Thakur, A. Mittal, Batch removal of hazardous azo dye Bismark Brown R using waste material hen feather, Ecol. Eng. 60 (2013) 249–253.
[30] A. Mittal, V. Thakur, V. Gajbe, Adsorptive removal of toxic azo dye Amido Black 10B by hen feather, Environ. Sci. Pollut. Res. 20 (2013) 260–269.
[31] B.H. Hameed, D.K. Mahmoud, A.L. Ahmad, Equilibrium modeling and kinetic studies on the adsorption of basic dye by a low-cost adsorbent: Coconut (*Cocos nucifera*) bunch waste, J. Hazard. Mater. 158 (2008) 65–72.
[32] R. Kumar, R. Ahmad, Biosorption of hazardous crystal violet dye from aqueous solution onto treated ginger waste (TGW), Desalination 265 (2011) 112–118.
[33] M.A.M. Salleh, D.K. Mahmoud, W.A. Karim, A. Idris, Cationic and anionic dye adsorption by agricultural solid wastes: A comprehensive review, Desalination 280 (2011) 1–13.
[34] I. Ozbay, U. Ozdemir, B. Ozbay, S. Veli, Kinetic, thermodynamic, and equilibrium studies for adsorption of azo reactive dye onto a novel waste adsorbent: Charcoal ash, Desalin. Water Treat. 51(31–33) (2013) 6091–6100.
[35] R. Ahmad, Studies on adsorption of crystal violet dye from aqueous solution onto coniferous pinus bark powder (CPBP), J. Hazard. Mater. 171 (2009) 767–773.
[36] A. Saeed, M. Sharif, M. Iqbal, Application potential of grapefruit peel as dye sorbent: Kinetics, equilibrium and mechanism of crystal violet adsorption, J. Hazard. Mater. 179 (2010) 564–572.
[37] O. Aksakal, H. Ucun, Equilibrium, kinetic and thermodynamic studies of the biosorption of textile dye (Reactive Red 195) onto *Pinus sylvestris* L., J. Hazard. Mater. 181 (2010) 666–672.
[38] M.J. Ahmed, S.K. Theydan, Microporous activated carbon from Siris seed pods by microwave-induced KOH activation for metronidazole adsorption, J. Anal. Appl. Pyrol. 99 (2013) 101–109.
[39] S. Largegren, About the theory of so-called adsorption of soluble substances, Kungliga Suensk Vetenskapsakademiens, Handlingar 241 (1898) 1–39.
[40] Y.S. Ho, G. McKay, Pseudo-second order model for sorption processes, Process Biochem. 34 (1999) 451–465.
[41] M.D. Low, Kinetics of chemisorption of gases on solids, Chem. Rev. 60 (1960) 267–312.
[42] W.J. Weber, J.C. Morris, Kinetics of adsorption on carbon from solutions, J. Sanit. Eng. Div. 89 (1963) 31–60.
[43] M.M. Nassar, M.S. El-Geundi, A.A. Al-Wahbi, Equilibrium modeling and thermodynamic parameters for adsorption of cationic dyes onto Yemen natural clay, Desalin. Water Treat. 44 (2012) 340–349.
[44] R. Baccar, P. Blánquez, J. Bouzid, M. Feki, H. Attiya, M. Sarrà, Modeling of adsorption isotherms and kinetics of a tannery dye onto an activated carbon prepared from an agricultural by-product, Fuel Process. Technol. 106 (2013) 408–415.
[45] M. Auta, B.H. Hameed, Preparation of waste tea activated carbon using potassium acetate as an activating agent for adsorption of Acid Blue 25 dye, Chem. Eng. J. 171 (2011) 502–509.
[46] R. Gong, S. Zhu, D. Zhang, J. Chen, S. Ni, R. Guan, Adsorption behavior of cationic dyes on citric acid esterifying wheat straw: Kinetic and thermodynamic profile, Desalination 230 (2008) 220–228.
[47] M. Berrios, M.A. Martín, A. Martín, Treatment of pollutants in wastewater: Adsorption of methylene blue onto olive-based activated carbon, J. Ind. Eng. Chem. 18 (2012) 780–784.
[48] O. Redlich, D.L. Peterson, A useful adsorption isotherm, J. Phys. Chem. 63 (1959) 1024–1024.
[49] Y. Ho, W. Chiu, C. Wang, Regression analysis for the sorption isotherms of basic dyes on sugarcane dust, Bioresour. Technol. 96 (2005) 1285–1291.

[50] P.S. Kumar, S. Ramalingam, C. Senthamarai, M. Niranjanaa, P. Vijayalakshmi, S. Sivanesan, Adsorption of dye from aqueous solution by cashew nut shell: Studies on equilibrium isotherm, kinetics and thermodynamics of interactions, Desalination 261 (2010) 52–60.
[51] M.J. Tempkin, V. Pyzhev, Kinetics of ammonia synthesis on promoted iron catalysts, Acta Physicochim. URSS 12 (1940) 217–222.
[52] C. Aharoni, M. Ungarish, Kinetics of activated chemisorption. Part 2. – Theoretical models, J. Chem. Soc., Faraday Trans. 73 (1977) 456–464.
[53] T. Madrakian, A. Afkhami, M. Ahmadi, Adsorption and kinetic studies of seven different organic dyes onto magnetite nanoparticles loaded tea waste and removal of them from wastewater samples, Spectrochim. Acta A. Mol. Biomol. Spectrosc. 99 (2012) 102–109.
[54] K.P. Singh, S. Gupta, A.K. Singh, S. Sinha, Optimizing adsorption of crystal violet dye from water by magnetic nanocomposite using response surface modeling approach, J. Hazard. Mater. 186 (2011) 1462–1473.
[55] G.R. Mahdavinia, H. Aghaie, H. Sheykhloie, M.T. Vardini, H. Etemadi, Synthesis of CarAlg/MMt nanocomposite hydrogels and adsorption of cationic crystal violet, Carbohydr. Polym. 98 (2013) 358–365.
[56] G.O. El-Sayed, Removal of methylene blue and crystal violet from aqueous solutions by palm kernel fiber, Desalination 272 (2011) 225–232.
[57] S. Jain, R.V. Jayaram, Removal of basic dyes from aqueous solution by low-cost adsorbent: Wood apple shell (*Feronia acidissima*), Desalination 250 (2010) 921–927.
[58] A.R. Khan, M.R. Riazi, Y.A. Al-Roomi, A thermodynamic model for liquid adsorption isotherms, Sep. Purif. Technol. 18 (2000) 237–250.
[59] H. Guedidi, L. Reinert, J. Lévêque, Y. Soneda, N. Bellakhal, L. Duclaux, The effects of the surface oxidation of activated carbon, the solution pH and the temperature on adsorption of ibuprofen, Carbon 54 (2013) 432–443.
[60] M. Kumar, R. Tamilarasan, V. Sivakumar, Adsorption of Victoria blue by carbon/Ba/alginate beads: Kinetics, thermodynamics and isotherm studies, Carbohydr. Polym. 98 (2013) 505–513.
[61] W. Zou, K. Li, H. Bai, X. Shi, R. Han, Enhanced cationic dyes removal from aqueous solution by oxalic acid modified rice husk, J. Chem. Eng. Data 56 (2011) 1882–1891.
[62] M. Ghaedi, A. Ansari, R. Sahraei, ZnS:Cu nanoparticles loaded on activated carbon as novel adsorbent for kinetic, thermodynamic and isotherm studies of Reactive Orange 12 and Direct yellow 12 adsorption, Spectrochim. Acta A Mol. Biomol. Spectrosc. 114 (2013) 687–694.